

# Chapter 14

## LANDAU DAMPING

As we have seen in previous chapters, collective instabilities occur in bunched and unbunched beam as a result of the interaction of the beam particles with their own wake fields. There are various way to damp these instabilities. Aside from mechanical dampers, there is a natural stabilization mechanism against collective instabilities when the beam particles have a small spread in their frequencies, such as betatron frequency, synchrotron frequency, or revolution frequency as the situation requires. This damping mechanism is called *Landau damping*, which was first formulated by Landau [1]. Unfortunately, Landau's original paper is rather difficult to understand. Later, Jackson [2] wrote an article on longitudinal plasma oscillations and had the concept well explained.

Neil and Sessler [3] first formulated the theory of Landau damping on longitudinal instabilities, while Laslett, Neil and Sessler [4] first applied the theory to transverse instabilities. There have been quite a number of good papers written on this subject by Hereward [5], Hofmann [6], and Chao [7].

We encountered Landau damping in Chapter 6 when we formulated the dispersion relation for longitudinal microwave instability using the Vlasov equation. There, we came across the ambiguity of a singularity in the denominator which is critical in determining whether the system will be stable or unstable. That ambiguity can only be avoided when the problem is treated as an initial-value problem. This will be covered in this chapter. We first study the beam response of an harmonic driving force, the beam response of shock or  $\delta$ -pulse excitation. After that, we try to understand the physics of Landau damping and derive dispersion relations for bunched and unbunched beam in transverse and longitudinal instabilities.

## 14.1 Harmonic Beam Response

Consider a particle having a natural angular frequency  $\omega$  and is driven by a force of angular frequency  $\Omega$ . The equation describing its displacement  $x(t)$  is

$$\ddot{x} + \omega^2 x = A \cos \Omega t , \quad (14.1)$$

where the overdot represents derivative with respect to time and  $A$  denotes the amplitude of the force. The most general solution is

$$x(t) = x_0 \cos \omega t + \dot{x}_0 \frac{\sin \omega t}{\omega} + \frac{A}{\omega^2 - \Omega^2} [\cos \Omega t - \cos \omega t] , \quad (14.2)$$

where  $x_0$  and  $\dot{x}_0$  are, respectively the initial value of  $x$  and  $\dot{x}$  at  $t = 0$ . The first two terms are due to a shock or  $\delta$ -pulse excitation. Although they are important, we shall postpone the discussion to the next section.

Let us pay attention to the excitation by the harmonic force. Notice that the response is well-behaved even at  $\omega = \Omega$ . For a large number of particles having a distribution  $\rho(\omega)$  in frequency and normalized to unity, the displacement of the center of mass is

$$\langle x(t) \rangle = A \int_{-\infty}^{\infty} d\omega \frac{\rho(\omega)}{\omega^2 - \Omega^2} [\cos \Omega t - \cos \omega t] . \quad (14.3)$$

As is the case in particle beams, the distribution is mostly a narrow one centered at angular frequency  $\bar{\omega}$ . For simplicity, let us assume that this distribution does not peak at any other frequency, not even the negative frequencies. In order to drive this system of particles, the driving frequency must also be close to this center frequency, or  $\Omega \approx \bar{\omega}$ . We can therefore do the expansion  $\omega = \Omega + (\omega - \Omega)$ , and the Eq. (14.3) can be approximated by

$$\langle x(t) \rangle = \frac{A}{2\bar{\omega}} \left[ \cos \Omega t \int_{-\infty}^{\infty} d\omega \rho(\omega) \frac{1 - \cos(\omega - \Omega)t}{\omega - \Omega} + \sin \Omega t \int_{-\infty}^{\infty} d\omega \rho(\omega) \frac{\sin(\omega - \Omega)t}{\omega - \Omega} \right] . \quad (14.4)$$

Notice that we have separated the fast-oscillating term of angular frequency  $\Omega$  and the slow-oscillating envelope-like terms with angular frequency  $\omega - \Omega$ . We also see a part, the  $\cos \Omega t$  term, that is not driven *in phase*\* by the force, and the other part, the  $\sin \Omega t$  term, that is driven in phase by the force. More discussion will follow later. The functions

$$p(\omega) = \frac{1 - \cos \omega t}{\omega} \quad \text{and} \quad d(\omega) = \frac{\sin \omega t}{\omega} \quad (14.5)$$

---

\*Actually, “in phase” here implies the driving phase is in phase with the velocity  $\dot{x}$ .

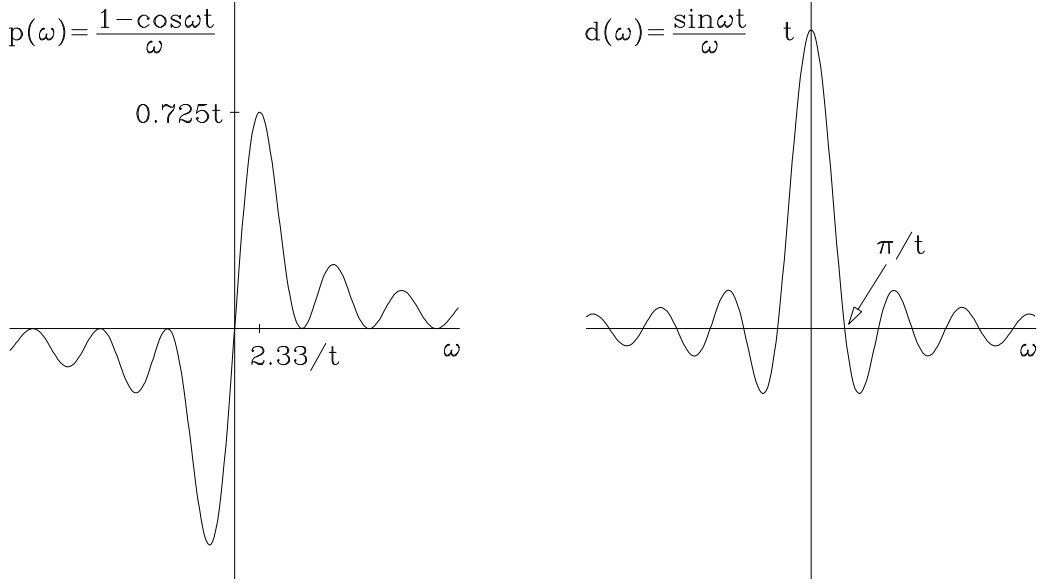


Figure 14.1: Plots of the functions  $p(\omega)$  and  $d(\omega)$  with  $t$  being a parameter. As  $t \rightarrow \infty$ ,  $p(\omega) \rightarrow \wp \omega^{-1}$  and  $d(\omega) \rightarrow \pi \delta(\omega)$ , where  $\wp$  denotes principal value.

are illustrated in Fig. 14.1. The function  $p(\omega)$  always vanishes at  $\omega = 0$  and decays as  $\omega^{-1}$  when  $\omega \rightarrow \pm\infty$ . It has peaks of value  $\pm at$  at  $\pm b/t$ , where  $b = 2.3311$  is the root of  $b = \tan(b/2)$  and  $a = 2b/(1 + b^2) = 0.7246$ . These peaks grow linearly with  $t$  and move closer to  $\omega = 0$  as  $t$  increases. We therefore have

$$\lim_{t \rightarrow \infty} p(\omega) = \wp \frac{1}{\omega}, \quad (14.6)$$

where  $\wp$  stands for the principal value. On the other hand,  $d(\omega)$  has a peak of value  $t$  at  $\omega = 0$  and rolls off as  $\omega^{-1}$  for large  $\omega$ , having the first zeroes at  $\omega = \pm\pi/t$ . As  $t \rightarrow \infty$ , the peak at  $\omega = 0$  grows linearly while its width also shrinks inversely with  $t$ ; the area enclosed is always  $\pi$ . Outside the peak, the function oscillates very fast as  $t \rightarrow 0$ . We therefore have

$$\lim_{t \rightarrow \infty} d(\omega) = \pi \delta(\omega). \quad (14.7)$$

Coming back to Eq. (14.4), as  $t \gg 1/\Delta\omega$ , where  $\Delta\omega$  is a measure of the width of the frequency distribution  $\rho(\omega)$ , all the transients die, leaving us with

$$\langle x(t) \rangle = \frac{A}{2\bar{\omega}} \left[ \cos \Omega t \wp \int_{-\infty}^{\infty} d\omega \frac{\rho(\omega)}{\omega - \Omega} + \pi \rho(\Omega) \sin \Omega t \right]. \quad (14.8)$$

Let now us repeat the derivation with the force  $A \sin \Omega t$  and combine the solution

with the former to get the long-term response to the force  $Ae^{-i\Omega t}$ :

$$\langle x(t) \rangle = \frac{Ae^{-i\Omega t}}{2\bar{\omega}} \left[ \wp \int_{-\infty}^{\infty} d\omega \frac{\rho(\omega)}{\omega - \Omega} + i\pi\rho(\Omega) \right] = \frac{Ae^{-i\Omega t}}{2\bar{\omega}\Delta\omega} R(u) , \quad (14.9)$$

where the beam transfer function (BTF) is defined as

$$R(u) = f(u) + ig(u) , \quad (14.10)$$

with

$$u = \frac{\bar{\omega} - \Omega}{\Delta\omega} , \quad (14.11)$$

and

$$f(u) = \Delta\omega \wp \int_{-\infty}^{\infty} d\omega \frac{\rho(\omega)}{\omega - \Omega} \quad \text{and} \quad g(u) = \pi\Delta\omega\rho(\bar{\omega} - u\Delta\omega) , \quad (14.12)$$

where again  $\Delta\omega$  is a measure of the width of the frequency distribution. The BTF is an important function, because it can be measured and it gives valuable information to the distribution function  $\rho(\omega)$  and also the impedance of the vacuum chamber, as will be demonstrated below. We can also combine the two expressions in Eq. (14.12) into one and obtain

$$R(u) = f(u) + ig(u) = \Delta\omega \int_{-\infty}^{\infty} d\omega \frac{\rho(\omega)}{\omega - \Omega - i\epsilon} \quad \text{with} \quad u = \frac{\bar{\omega} - \Omega}{\Delta\omega} . \quad (14.13)$$

There is a singularity in  $R(u)$  when  $\Omega = \omega - i\epsilon$  or  $u\Delta\omega = \bar{\omega} - \omega + i\epsilon$ . This implies that  $R(u)$  is an analytic function with singularities only in the upper  $u$ -plane. Notice that instead of the derivation starting from the initial condition, the displacement of the center of the bunch, Eq. (14.9), can also be obtained directly by writing the force as

$$Ae^{-i(\Omega+i\epsilon)t} = Ae^{-i\Omega t}e^{\epsilon t} , \quad (14.14)$$

where  $\epsilon$  is an infinitesimal positive number, so that the solution becomes

$$\langle x(t) \rangle = \frac{Ae^{-i\Omega t}}{2\bar{\omega}} \int_{-\infty}^{\infty} d\omega \frac{\rho(\omega)}{\omega - \Omega - i\epsilon} = \frac{Ae^{-i\Omega t}}{2\bar{\omega}} \left[ \wp \int_{-\infty}^{\infty} d\omega \frac{\rho(\omega)}{\omega - \Omega} + i\pi\rho(\Omega) \right] , \quad (14.15)$$

which is exactly the same as Eq. (14.9). The addition of the small  $\epsilon$  implies that the force in Eq. (14.14) is zero at  $t = -\infty$  and increases adiabatically.

## 14.2 Shock Response

The beam is suddenly excited by a shock or a  $\delta$ -pulse, imparting to the beam particles either a displacement  $x_0$  or a velocity displacement  $\dot{x}_0$ , but not both. From Eq. (14.2), we have the shock response defined by either

$$G(t) = \frac{\langle x(t) \rangle}{x_0} = H(t) \int_{-\infty}^{\infty} d\omega \rho(\omega) \cos \omega t , \quad (14.16)$$

or

$$G(t) = \frac{\langle \dot{x}(t) \rangle}{\dot{x}_0} = H(t) \int_{-\infty}^{\infty} d\omega \rho(\omega) \cos \omega t , \quad (14.17)$$

where  $H(t)$  is the Heaviside step function. Thus the shock response function (SRF) is always real and vanishes when  $t < 0$ . The SRF is important because it is an easily measured function and it can give information about the distribution function of the frequency as well as the BTF.

It is interesting to show that there is a relation between the the SRF and the BTF. The Fourier transform of the SRF is

$$\tilde{G}(\omega) = \frac{1}{2\pi} \int_0^{\infty} dt G(t) e^{i\omega t} . \quad (14.18)$$

where attention has to be paid that the integral starts from zero. The real part is

$$\begin{aligned} \mathcal{R}e \tilde{G}(\omega) &= \frac{1}{2\pi} \int_0^{\infty} dt G(t) \cos \omega t \\ &= \frac{1}{2\pi} \int_0^{\infty} dt \cos \omega t \int_{-\infty}^{\infty} d\omega' \rho(\omega') \cos \omega' t \\ &= \frac{1}{4\pi} \int_{-\infty}^{\infty} d\omega' \rho(\omega') \int_{-\infty}^{\infty} dt \cos \omega t \cos \omega' t \\ &= \frac{1}{4} \int_{-\infty}^{\infty} d\omega' \rho(\omega') [\delta(\omega' - \omega) + \delta(\omega' + \omega)] \\ &= \frac{1}{4} \rho(\omega) , \end{aligned} \quad (14.19)$$

where  $\delta(\omega' + \omega)$  has no contribution because the distribution is narrow and is centered

at only one positive frequency. The imaginary part is

$$\begin{aligned}
\text{Im } \tilde{G}(\omega) &= \frac{1}{2\pi} \int_0^\infty dt G(t) \sin \omega t \\
&= \frac{1}{2\pi} \int_0^\infty dt \sin \omega t \int_{-\infty}^\infty d\omega' \rho(\omega') \cos \omega' t \\
&= \frac{1}{4\pi} \int_{-\infty}^\infty d\omega' \rho(\omega') \int_0^\infty dt \left[ \sin(\omega - \omega')t + \sin(\omega + \omega')t \right] \\
&= \frac{1}{4\pi} \left[ \wp \int_{-\infty}^\infty d\omega' \frac{\rho(\omega')}{\omega - \omega'} + \wp \int_{-\infty}^\infty d\omega' \frac{\rho(\omega')}{\omega + \omega'} \right]
\end{aligned} \tag{14.20}$$

where again the last principal-value integral involving  $\omega + \omega'$  can be neglected because of the narrow spread of the distribution  $\rho$ . We write these integrals as principal-value integrals because during the derivation, one integrand vanishes when  $\omega' - \omega = 0$  and the other vanishes when  $\omega + \omega' = 0$ . Combining the result,

$$\begin{aligned}
\tilde{G}(\omega) &= \frac{-i}{4\pi} \left[ \wp \int_{-\infty}^\infty d\omega' \frac{\rho(\omega')}{\omega' - \omega} + i\pi\rho(\omega) \right] \\
&= \frac{-i}{4\pi\Delta\omega} \left[ f(u) + ig(u) \right] = \frac{-i}{4\pi\Delta\omega} R(u)
\end{aligned} \tag{14.21}$$

In other words, the Fourier transform of the SRF is equal to the BTF multiplied by  $-i/(4\pi\Delta\omega)$ . This also provides us with a way to compute the BTF. The procedure is: compute the SRF  $G(t)$ , find its Fourier transform  $\tilde{G}(\omega)$ , and then infer the BTF  $R(u)$ .

As an example, take the Lorentz distribution

$$\rho(\omega) = \frac{\Delta\omega}{\pi} \frac{1}{(\omega - \bar{\omega})^2 + (\Delta\omega)^2}. \tag{14.22}$$

The SRF is

$$\begin{aligned}
G(t) &= H(t) \mathcal{R}e \int_{-\infty}^\infty d\omega \frac{\Delta\omega}{\pi} \frac{e^{i\omega t}}{(\omega - \bar{\omega})^2 + (\Delta\omega)^2} \\
&= H(t) \mathcal{R}e e^{i(\bar{\omega} + i\Delta\omega)t} = H(t) e^{-\Delta\omega t} \cos \bar{\omega}t
\end{aligned} \tag{14.23}$$

Next the Fourier transform,

$$\begin{aligned}
\tilde{G}(\omega) &= \frac{1}{2\pi} \int_0^\infty dt \cos \bar{\omega} t e^{(-\Delta\omega+i\omega)t} \\
&= \frac{1}{4\pi} \int_0^\infty dt [e^{i(\bar{\omega}+i\Delta\omega+\omega)t} + e^{i(-\bar{\omega}+i\Delta\omega+\omega)t}] \\
&= \frac{1}{4\pi} \left[ \frac{1}{-i(\bar{\omega}+\omega+i\Delta\omega)} + \frac{1}{i(\bar{\omega}-\omega-i\Delta\omega)} \right] \\
&= \frac{-i}{4\pi\Delta\omega} \frac{1}{u-i} = \frac{-i}{4\pi\Delta\omega} \frac{u+i}{u^2+1}, \tag{14.24}
\end{aligned}$$

where again the smaller term involving  $\omega_r + \omega$  has been removed. Thus the BTF is

$$R(u) = f(u) + ig(u) = \frac{u+i}{u^2+1}, \tag{14.25}$$

which is equal to the Fourier transform of the SRF  $G(t)$  multiplied by  $-i/(4\pi\Delta\omega)$ . These results are depicted in Fig. 14.2. As expected the shock excitation is the decay of the center displacement  $\langle x \rangle$  or the center velocity displacement  $\langle \dot{x} \rangle$ . The decay comes from the distribution  $\rho(\omega)$  so that each particle oscillates with a slightly different frequency. The particles will spread out and therefore the decay of the center displacement or the center velocity displacement. This is usually known as *decoherence* or *filamentation*. For the Lorentz distribution, the decay turns out to be exponential. However, it is important to point out that the center  $\langle \dot{x} \rangle$  decays because initially we have a nonzero  $x_0$  but  $\dot{x}_0 = 0$ . In case  $\dot{x}_0 \neq 0$ , the Lorentz distribution *does not* give a decay of the center displacement, (Exercise 14.1).

Table 14.1 lists the BTF and SRF for some commonly used frequency distributions (Exercise 14.2): the Lorentz distribution, the rectangular distribution, the parabolic distribution, the elliptical distribution, the bi-Lorentz distribution, and the Gaussian distribution.

Because the BTF is the Fourier transform of SRF,  $G(t)$  is also the inverse Fourier transform of  $R(u)$ :

$$G(t) = \mathcal{Re} \frac{-i}{4\pi\Delta\omega} \int_{-\infty}^{\infty} d\omega R \left( \frac{\bar{\omega} - \omega}{\Delta\omega} \right) e^{-i\omega t}. \tag{14.26}$$

The  $\mathcal{Re}$  should not be there. It is there because we have consistently neglected the frequencies around  $-\bar{\omega}$ .

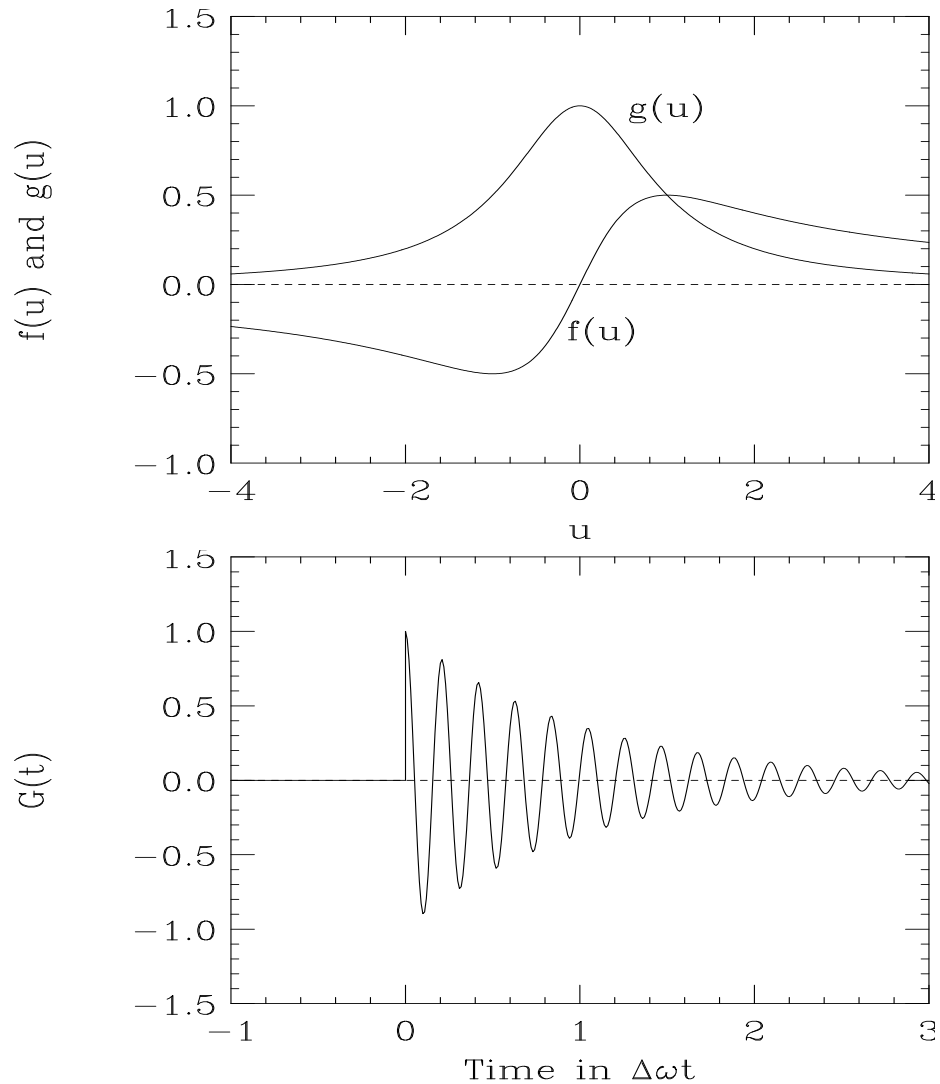


Figure 14.2: For Lorentz frequency distribution, plots showing beam transfer function  $R(u) = f(u) + ig(u)$  (top) and shock response function  $G(t)$  (bottom).

Table 14.1: Shock excitation function  $G(t)$  and beam transfer function  $R(u) = f(u) + ig(u)$  for various frequency distributions  $\rho(\omega)$  with  $v = (\omega_x - \omega)/\Delta\omega$ .

Frequency Distribution		Shock Response $G(t)$	Beam response function	
Type	Distribution		$f(u)$	$g(u)$
Lorentz	$\frac{1}{\pi\Delta\omega} \frac{1}{v^2+1}$	$e^{-\Delta\omega t} \cos \omega_x t$	$\frac{u}{u^2+1}$	$\frac{1}{u^2+1}$
rectangular	$\frac{1}{2\Delta\omega} H(1- v )$		$\frac{1}{2} \ln \left  \frac{u+1}{u-1} \right $	$\frac{\pi}{2} H(1- u )$
parabolic	$\frac{3}{4\Delta\omega} (1-v^2) H(1- v )$		$\frac{3}{4} \left[ (1-u^2) \ln \left  \frac{u+1}{u-1} \right  + 2u \right]$	$\frac{3\pi}{4} (1-u^2) H(1- v )$
elliptical	$\frac{2}{\pi\Delta\omega} \sqrt{1-v^2} H(1- v )$		$2 \left[ u - \text{sgn}(u) \sqrt{1-u^2} H(1- u ) \right]$	$2\sqrt{1-u^2} H(1- u )$
bi-Lorentz	$\frac{2}{\pi\Delta\omega} \frac{1}{(v^2+1)^2}$		$\frac{u(u^2+3)}{(u^2+1)^2}$	$\frac{2}{(u^2+1)^2}$
Gaussian	$\frac{1}{\sqrt{2\pi\Delta\omega}} e^{-v^2/2}$	$e^{-(\Delta\omega t)^2/2} \cos \omega_x t$	$\sqrt{\frac{2}{\pi}} e^{-u^2/2} \int_0^\infty \frac{dy}{y} e^{-y^2/2} \sinh uy$	$\sqrt{\frac{\pi}{2}} e^{-u^2/2}$

### 14.3 Landau Damping

After understanding the BTF and the SRF, let us come back to the transient response of a harmonic excitation; i.e., Eq. (14.4). The term proportional to  $\sin \Omega t$  is driven in phase by the harmonic force, and the particle should be absorbing energy. Let us rewrite Eq. (14.3) in the approximation that the frequency distribution  $\rho(\omega)$  is narrow around  $\bar{\omega}$ :

$$\langle x(t) \rangle = \frac{A \sin \bar{\omega} t}{\bar{\omega}} \int_{-\infty}^{\infty} d\omega \rho(\omega) \frac{\sin \frac{1}{2}(\omega - \Omega)t}{\omega - \Omega}. \quad (14.27)$$

Consider a component corresponding to the frequency  $\omega$ , its envelope is

$$\text{Amplitude}(\omega) = \frac{A}{\bar{\omega}} \frac{\sin \frac{1}{2}(\omega - \Omega)t}{\omega - \Omega}. \quad (14.28)$$

This means that all particles having frequency  $\omega$  are excited at  $t = 0$ , increase to a maximum of  $A/[\bar{\omega}(\omega - \Omega)]$  at  $t \approx \pi/(\omega - \Omega)$ , and die down to zero again at  $t = 2\pi/(\omega - \Omega)$ . Thus, energy is gained but is given back to the system. For  $\omega$  closer to  $\Omega$ , the response amplitude rises to a larger amplitude and the energy is given back to the system at a later time. For those particles that have exactly frequency  $\Omega$ , the amplitude grows linearly with time and the energy keeps on growing. This is called *Landau damping*. An illustration is shown in Fig. 14.3, where the solid curve shows a particle having exactly the same frequency as  $\Omega$  and growing linearly, while the dashed curve shows a particle with frequency 95% of  $\Omega$  decaying after about 10 oscillations. In other words, particles with  $\omega$  far away from  $\Omega$  get excited, but the energy is returned to those particles having  $\omega$  close to  $\Omega$ , which are still absorbing energy. As time increases, particles with frequencies closer to  $\Omega$  give up their energies to particles with frequencies much closer to  $\Omega$ . Thus, as time progresses, less and less particles are still absorbing energy. As  $t \rightarrow \infty$ , only particles with frequency exactly equal to  $\Omega$  will be absorbing energy, and there are only very few particles doing this. So particles with frequencies very close to  $\Omega$  will have their amplitudes keep on increasing. In practice, when these growing amplitudes hit the vacuum chamber, the process will stop. This sets the time limit for Landau damping to stop. The damping process starts when the amplitude of the first particle is damped and this time is  $t \approx 2\pi/\Delta\omega$ .

Let us study the energy in the system. The energy is proportional to the square of the amplitude. Therefore the energy of all the particles is

$$\mathcal{E} = \frac{NA^2}{\bar{\omega}^2} \int_{-\infty}^{\infty} d\omega \rho(\omega) \frac{\sin^2(\omega - \Omega)t/2}{(\omega - \Omega)^2}, \quad (14.29)$$

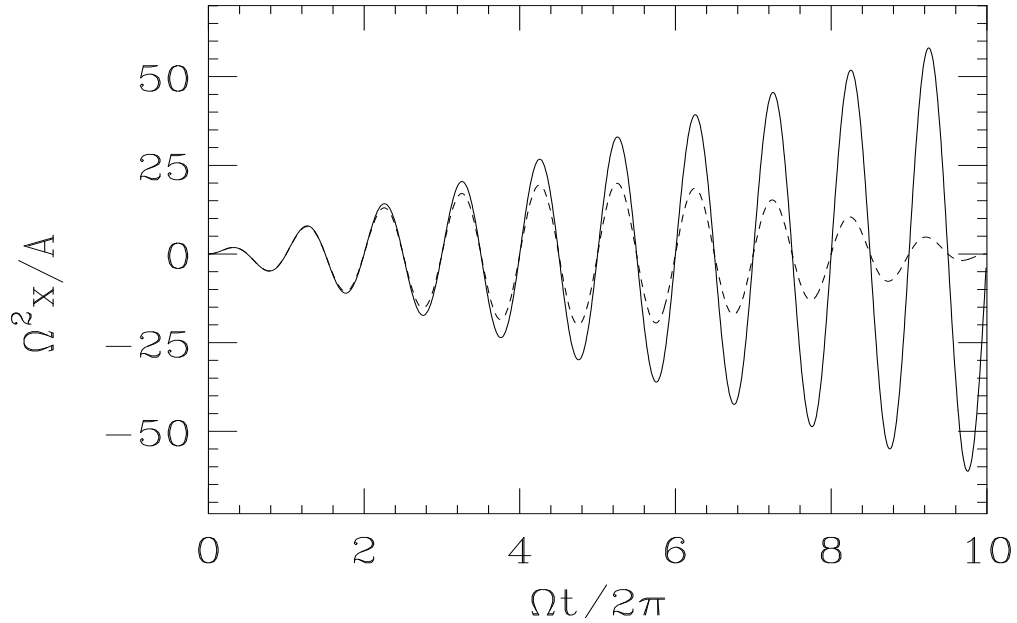


Figure 14.3: Solid: the response of a particle having exactly the same frequency  $\Omega$  as the driving force grows linearly in time. Dashes: the response of a particle having frequency 95% of  $\Omega$  gives up its energy after about 10 oscillations.

where  $N$  is the total number of beam particles in the system. We see that as time progresses the amplitude square,

$$\text{Amplitude}(\omega)^2 = \frac{\sin^2(\omega - \Omega)t/2}{(\omega - \Omega)^2}, \quad (14.30)$$

becomes sharper and sharper while its width shrinks. This verifies that energy is being transferred by the particles having frequencies far away from  $\Omega$  to particles having frequencies closer to  $\Omega$ . Since the square of the amplitude always has an area of  $\pi t/2$ , we have

$$\lim_{t \rightarrow \infty} \text{Amplitude}(\omega)^2 = \lim_{t \rightarrow \infty} \frac{\sin^2(\omega - \Omega)t/2}{(\omega - \Omega)^2} = \frac{\pi t}{2} \delta(\omega - \Omega). \quad (14.31)$$

Thus, at  $t \rightarrow \infty$ , the steady-state energy of the system is

$$\mathcal{E} = \frac{\pi}{2} \frac{NA^2}{\bar{\omega}^2} \rho(\Omega)t, \quad (14.32)$$

which increases linearly with time, and all this energy goes into those few particles having exactly the same frequency as  $\Omega$ . However, we do see in the asymptotic solution of Eq. (14.8) that  $\langle x(t) \rangle$  does not go to infinity. This is not a contradiction, because

even when a few particles have very large and still growing amplitudes, the centroid will not be affected.

In our study so far, the amplitude  $A$  of the driving force is independent of the system of particles. For an instability in a particle beam, the situation is slightly different. The driving force comes from the wake fields of the beam particles interacting with the discontinuities of the vacuum chamber, and usually has an amplitude proportional to the center displacement of the beam. When there is a kick to the beam that creates a center displacement  $\langle x(0) \rangle$  or a center displacement velocity  $\langle \dot{x}(0) \rangle$ , a force with amplitude  $A \propto \langle x(0) \rangle$  or  $\langle \dot{x}(0) \rangle$  is generated and drives the whole system of particles with the coherent frequency  $\Omega$ . Each frequency component of the beam will receive the amount of response according to Eq. (14.28). Now two things happen. First, the particles give up their excited energy gradually to those particles having frequencies extremely close to  $\Omega$ , the frequency of the driving force, and the center of displacement approaches the BTF  $R(u)$ . Second, the center of displacement of the beam starts to decay according to the SRF  $G(t)$ . As  $\langle x(t) \rangle$  decreases, the driving force decreases also. Finally, the disturbance goes away. This is how Landau damping takes place in a beam. In fact, this process starts whenever the disturbance is of infinitesimal magnitude. This implies that any disturbance will be damped as soon as it occurs. We say that there will be enough Landau damping to keep the beam stable. Notice that no frictional force has ever been introduced in the discussion. Thus, there is still conservation of energy in the presence of Landau damping, which merely redistributes energy from waves of one frequency to another.

In case the frequency spread  $\Delta\omega$  is very very narrow, it will take  $t \approx \pi/\Delta\omega$  for the first wave to surrender its energy to another that has frequency closer to  $\Omega$ . This time will be very long. Before this time arrives, all frequency components continue to receive energy and  $\langle x(t) \rangle$  increases and so will be the driving force. This is the picture of how an instability develops when the spread of frequency is not large enough to invoke Landau damping. However, the conservation of energy still holds. The energy that feeds the instability may be extracted from the longitudinal kinetic energy of the beam resulting in a slower speed, or from the rf system that replenish the beam energy.

## 14.4 Transverse Bunched Beam Instabilities

Consider a bunch with infinitesimal longitudinal length but with finite transverse extent. We call this a slice bunch. We want to study its transverse motion. The frequency of interest here is the betatron frequency  $\omega_\beta$  which has the incoherent tune shift included. The equation of motion of a particle with transverse displacement  $y$  is

$$\frac{d^2y}{ds^2} + \frac{\omega_\beta^2}{v^2}y = \frac{\langle F(\bar{y}) \rangle}{\gamma m \beta^2 c^2}, \quad (14.33)$$

where  $v = \beta c$  is the particle longitudinal velocity and  $\bar{y}$  is the average displacement of the bunch (sometimes we use the notation  $\langle y \rangle$ ). This is the same as Eq. (4.4) in Chapter 4, but with the average wake force linear in  $y$  absorbed into  $\omega_\beta^2$ . The force on the right side of Eq. (14.33) is related to the transverse wake function,

$$\langle F(\bar{y}) \rangle = -\frac{e^2 N}{C} \sum_{k=1}^{\infty} \bar{y}(s - kC) W_1(kC) \quad (14.34)$$

where the summation is over previous turns. The negative sign shows that the force is opposing the displacement. Because this is a slice bunch, the wake force can only come from the passage of the same bunch in previous turns. Let us denote a collective excitation of the dipole moment  $D$  of the bunch center  $\bar{y}(s)$  at the collective frequency  $\Omega$  by the ansatz

$$\bar{y}(s) = D e^{-i\Omega s / (\beta c)}, \quad (14.35)$$

where  $\Omega \rightarrow \Omega + i\epsilon$  is assumed. Expressing in terms of the transverse impedance  $Z_1^\perp$ , Eq. (14.33) becomes

$$\frac{d^2y}{ds^2} + \frac{\omega_\beta^2}{v^2}y = \frac{i e^2 N D}{\gamma m c C^2} \sum_{p=-\infty}^{\infty} Z_1^\perp(\Omega + p\omega_0) e^{-i\Omega s / (\beta c)}. \quad (14.36)$$

If we average the equation over all the particles in the bunch, we get the equation of motion of the center of the bunch,  $\bar{y}$ , and therefore the *coherent* betatron tune shift

$$(\Delta\omega_\beta)_{coh} = -\frac{i e^2 N \beta^2 c \mathcal{Z}_\perp}{2\omega_\beta \gamma m C^2}, \quad (14.37)$$

where we have introduced a short-hand form for the impedance

$$\mathcal{Z}_\perp = \sum_{p=-\infty}^{\infty} Z_1^\perp(\Omega + p\omega_0). \quad (14.38)$$

The imaginary part of the impedance contributes a real coherent tune shift. However, when  $\Re \mathcal{Z}_\perp < 0$ , the coherent tune shift has a positive imaginary part and the bunch will be unstable. If the driving impedance is narrow and covers less than one revolution harmonic centering roughly at  $q\omega_0$ , only two terms,  $p = \pm q$ , survive and Eq. (14.38) becomes

$$\Re \mathcal{Z}_\perp \approx \Re Z_1^\perp [(q + [\nu_\beta])\omega_0] - \Re Z_1^\perp [(q - [\nu_\beta])\omega_0], \quad (14.39)$$

where  $[\nu_\beta]$  denotes the residual or decimal part of the betatron tune. The bunch will be stable/unstable if the impedance peaks above/below  $q\omega_0$  giving an example of Robinson Instability in the transverse plane. The above summarizes what we have learned before without Landau damping.

Now let us introduce a distribution  $\rho(\omega_\beta)$  for the betatron frequency among the beam particles. This distribution is centered at  $\bar{\omega}_\beta$  with a spread  $\Delta\omega$ . The solution of Eq. (14.36) becomes

$$\begin{aligned} \bar{y}(s) &= \frac{ie^2 ND\beta^2 c \mathcal{Z}_\perp}{2\bar{\omega}_\beta \gamma m C^2} e^{-i\Omega s / (\beta c)} \int_{-\infty}^{\infty} d\omega_\beta \frac{\rho(\omega_\beta)}{\omega_\beta - \Omega - i\epsilon} \\ &= \frac{ie^2 ND\beta^2 c \mathcal{Z}_\perp}{2\bar{\omega}_\beta \Delta\omega \gamma m C^2} e^{-i\Omega s / (\beta c)} R(u), \end{aligned} \quad (14.40)$$

where the relation has been made to the BTF  $R(u)$  with  $u = (\bar{\omega}_\beta - \Omega) / \Delta\omega$ . If the ansatz of Eq. (14.35) is employed for  $\bar{y}(s)$ , we obtain

$$\frac{ie^2 N \beta^2 c \mathcal{Z}_\perp}{2\bar{\omega}_\beta \Delta\omega \gamma m C^2} = \frac{1}{R(u)}, \quad (14.41)$$

or

$$-\frac{(\Delta\omega_\beta)_{coh}}{\Delta\omega} = \frac{1}{R(u)}. \quad (14.42)$$

This is an equation of the coherent frequency  $\Omega$ . Given the impedance  $\mathcal{Z}_\perp$ , the left side is a constant and  $\Omega$  can be solved. More practically, we start with a fixed  $\Im \Omega$ , and solve for the impedance  $\mathcal{Z}$  while varying  $\Re \Omega$ . The result plotted in the complex impedance plane will be a contour for a fixed growth rate. In particular, we are interested in the contour for the threshold when  $\Im \Omega = 0+$ . This will be exactly the same as the loci of  $\Re u$  in the complex  $1/R(u)$  plane with  $\Im u = 0$ . Such threshold contours are plotted in Fig. 14.4 for various distributions. Remember that instability is generated by  $\Omega \rightarrow \Omega + i\epsilon$  with  $\epsilon$  real and positive. This translates to  $u \rightarrow u - i\epsilon$ . For the Lorentz distribution,

$$\frac{1}{R(u)} = u - i, \quad (14.43)$$

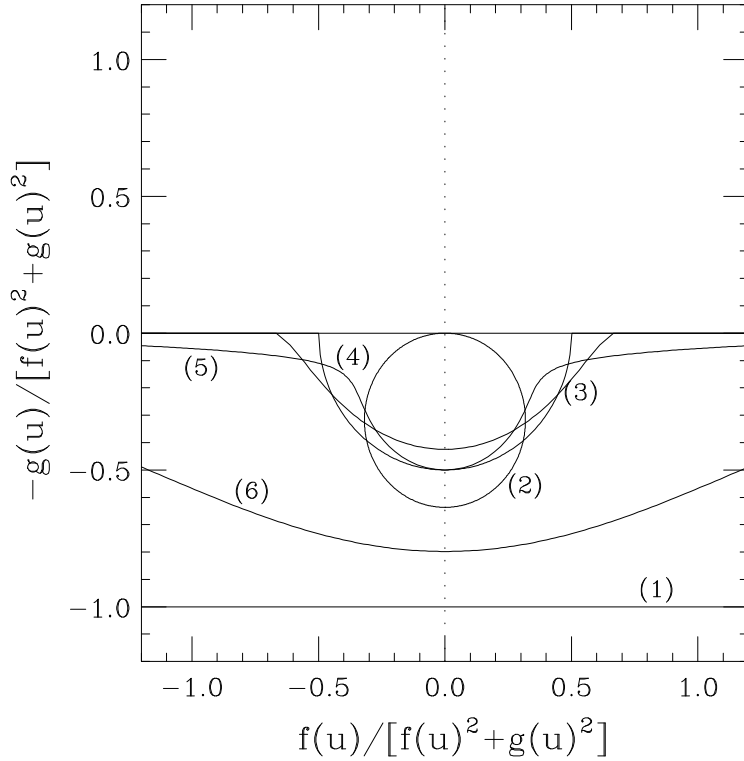


Figure 14.4: Threshold curves in the  $1/R(u)$  plane, where in every case the stability region is to the top of the curve and the instability region to the bottom. (1) Lorentz distribution, (2) rectangular distribution (a circle touching the  $V$ -axis), (3) parabolic distribution, (4) elliptical distribution (part of the dashed circle centered at origin), (5) bi-Lorentz distribution, (6) Gaussian distribution.

and it will be unstable if

$$\frac{1}{R(\mathcal{R}e u - i\epsilon)} = \mathcal{R}e u - i(1 + \epsilon). \quad (14.44)$$

Therefore the unstable region is below  $\mathcal{I}m R(u)^{-1} = -i$ , while the stable region is above  $\mathcal{I}m R(u)^{-1} = -1$ . Since the various distributions have been introduced with all different definitions of frequency spread  $\Delta\omega$ , Fig. 14.4 is not a good plot for the comparison of various distributions. Instead, we would like to reference everything with respect to the HWHM frequency spread  $\Delta\omega_{\text{HWHM}}$ . Thus, we define a new variable  $x$  to replace  $u$ :

$$u = xS \quad \text{with} \quad S = \frac{\Delta\omega_{\text{HWHM}}}{\Delta\omega}. \quad (14.45)$$

Equation (14.42) is rewritten as

$$-\frac{(\Delta\omega_\beta)_{\text{coh}}}{\Delta\omega_{\text{HWHM}}} = \frac{1}{\hat{R}(x)} . \quad (14.46)$$

where

$$\hat{R}(x) = \hat{f}(x) + i\hat{g}(x) = [f(u) + ig(u)]S . \quad (14.47)$$

It is customary to call the left side of Eq. (14.46)  $-i(U + iV)$ , following the counterpart in longitudinal microwave threshold, or

$$U + iV = \frac{i}{\hat{R}(x)} = \frac{i\hat{f}(x) + \hat{g}(x)}{\hat{f}^2(x) + \hat{g}^2(x)} . \quad (14.48)$$

so that  $U \propto -\mathcal{Re} Z_\perp$  and  $V \propto -\mathcal{Im} Z_\perp$ . The threshold curves for various frequency distributions are plotted in Fig. 14.5. Thus, whatever values of  $(U, V)$  lie to the left of the locus will be stable and whatever is on the right will be unstable. Without Landau damping, any  $U > 0$ , which implies betatron frequency shift with a positive imaginary part, will be unstable. Now, with Landau damping, the threshold has shifted to, for example,  $U = 1$  for the Lorentz distribution. There is one point on the stability curve that is simple to obtain. It is the point at  $x = 0$ . There  $\hat{f}(x) = 0$ , so that  $V = 0$  and  $U = 1/\hat{g}(0)$ . This point is important because it gives a rough idea of the threshold of instability. Similar to the Keil-Schnell stability circle for longitudinal microwave stability, we try to enclose the stability region in the  $U$ - $V$  plane by a circle of radius  $\frac{1}{\sqrt{3}}$ , which is shown in Fig. 14.5 as a dashed circle. This threshold circle coincides with the semi-circle of the elliptical distribution. Thus, the stability limit can be written as

$$|(\Delta\omega_\beta)_{\text{coh}}| \lesssim \frac{1}{\sqrt{3}} (\Delta\omega_\beta)_{\text{HWHM}} F , \quad (14.49)$$

where  $F$  is a form factor depending on the distribution and is equal to unity for the elliptical distribution. Form factors for various distributions are tabulated in Table 14.2 (Exercise 14.3). Figure 14.5 shows how far a frequency distribution has its instability threshold deviated from the Keil-Schnell type circle of Eq. (14.49). We see that the deviation of  $F$  from unity or the threshold curve from the Keil-Schnell circle increases as the distribution goes from elliptical, parabolic, rectangular, Gaussian, bi-Lorentz, to Lorentz.

Thus, a betatron tune spread can provide Landau damping for instabilities driven by the discontinuities of the vacuum chamber, provided that the driving impedance is not

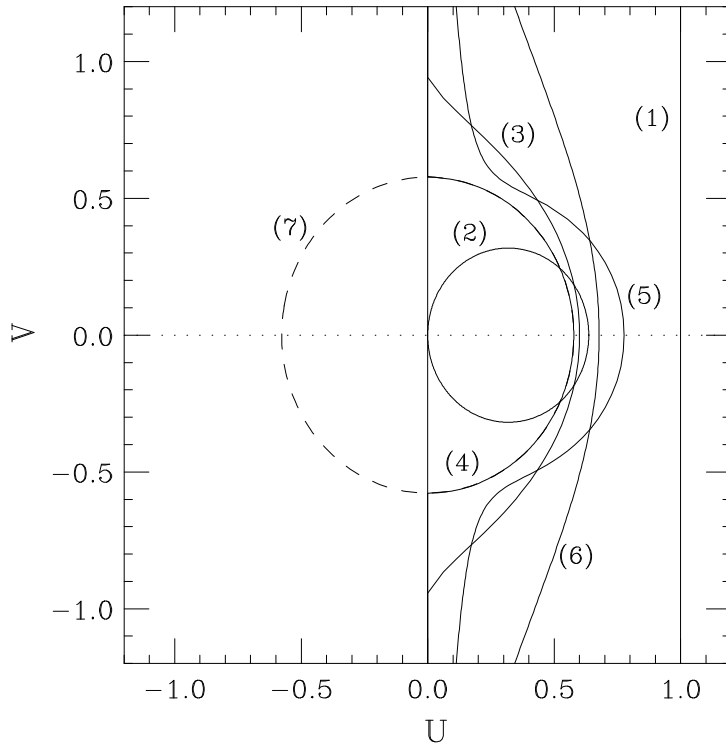


Figure 14.5: Threshold curves in the  $U$ - $V$  plane plotted with reference to the HWHM frequency spread. In every case the stability region is to the left of the curve and the instability region to the right. (1) Lorentz distribution, (2) rectangular distribution (a circle touching the  $V$ -axis), (3) parabolic distribution, (4) elliptical distribution (part of the dashed circle centered at origin), (5) bi-Lorentz distribution, (6) Gaussian distribution. The Keil-Schnell type stability circle is depicted in dashes by (7).

too large. The transverse mode-mixing or mode-coupling instabilities that we studied in Chapter 13 have not had Landau damping included. However, mode-coupling instability involves the coherent shifting of a betatron spectral line by as much as the synchrotron frequency. In order for Landau damping to work, a betatron tune spread of the order of the synchrotron frequency will be necessary. This amount of tune spread is quite simple for proton machines where the synchrotron tune is of the order  $\nu_s \sim 0.001$ . This provides for another explanation why transverse mode-mixing instabilities are usually not seen in proton machines. On the other hand, the synchrotron tunes for electron machines are usually  $\nu_s \sim 0.01$ . A betatron tune spread of this size is considered too large. For this reason, transverse mode-mixing instabilities in electron machines are usually alleviated by reactive dampers instead.

Table 14.2:  $U$ -intercept and form factor  $F$  defined in Eq. (14.49) for various distributions.

Distribution	$g(0)^{-1}$	$S = \frac{(\Delta\omega_\beta)_{\text{HWHM}}}{\Delta\omega}$	$U$ -intercept $\hat{g}(0)^{-1} = g(0)^{-1}S^{-1}$	Form factor $F = \sqrt{3}\hat{g}(0)^{-1}$
Lorentz	1	1	1	$\sqrt{3}$
rectangular	$\frac{2}{\pi}$	1	$\frac{2}{\pi}$	$\frac{2\sqrt{3}}{\pi}$
parabolic	$\frac{4}{3\pi}$	$\frac{1}{\sqrt{2}}$	$\frac{4\sqrt{2}}{3\pi}$	$\frac{4}{\pi}\sqrt{\frac{2}{3}}$
elliptical	$\frac{1}{2}$	$\frac{\sqrt{3}}{2}$	$\frac{1}{\sqrt{3}}$	1
bi-Lorentz	$\frac{1}{2}$	$\sqrt{\sqrt{2}-1}$	$\frac{1}{2\sqrt{\sqrt{2}-1}}$	$\frac{1}{2}\sqrt{\frac{3}{\sqrt{2}-1}}$
Gaussian	$\sqrt{\frac{2}{\pi}}$	$\sqrt{2\ln 2}$	$\frac{1}{\sqrt{\pi\ln 2}}$	$\sqrt{\frac{3}{\pi\ln 2}}$

## 14.5 Longitudinal Bunched Beam Instabilities

In a bunch, Landau damping proceeds through the spread in synchrotron frequency. Consider a short bunch consisting of  $N$  particles. The arrival time  $\tau$  ahead of the synchronous particle is governed by the equation of motion

$$\begin{aligned} \frac{d^2\tau}{ds^2} + \frac{\omega_s^2}{v^2}\tau &= \frac{e^2 N \eta}{v \beta^2 E_0 C} \sum_{k=-\infty}^{\infty} W'_0 [kT_0 + \bar{\tau}(s - kC) - \bar{\tau}(s)] \\ &= \frac{e^2 N \eta}{v \beta^2 E_0 C} \sum_{k=-\infty}^{\infty} [\bar{\tau}(s - kC) - \bar{\tau}(s)] W''_0(kT_0), \end{aligned} \quad (14.50)$$

where  $v = \beta c$  is the particle velocity, and a Taylor's expansion has been made because the amplitude of synchrotron oscillation is much smaller than the circumference of the ring. Comparing with Eq. (9.42), we have ignored the wake field within the bunch because the bunch is very short, and only included the effects from the bunch passage

through a fixed location of the accelerator ring in previous turns. Introduce the ansatz

$$\bar{\tau}(s) = Be^{-i\Omega s/v} , \quad (14.51)$$

with  $\Omega$  being the collective angular frequency to be determined. We next go to the frequency domain by introducing the longitudinal impedance  $Z_0^{\parallel}$ . Equation (14.50) can be written as

$$\frac{d^2\tau}{ds^2} + \frac{\omega_s^2}{v^2}\tau = -\frac{ie^2N\eta B\omega_0 Z_{\parallel}}{\beta^2 E_0 C^2} e^{-i\Omega s/v} , \quad (14.52)$$

where we have used and the short-hand notation

$$Z_{\parallel} = \sum_{p=-\infty}^{\infty} \left[ \left( p + \frac{\Omega}{\omega_0} \right) Z_0^{\parallel}(p\omega_0 + \Omega) - p Z_0^{\parallel}(p\omega_0) \right] . \quad (14.53)$$

Averaging Eq. (14.52) over all the particles in the bunch, we obtain the equation of motion for the center of the bunch, and therefore the *coherent* synchrotron frequency shift

$$(\Delta\omega_s)_{\text{coh}} = \Omega - \omega_s = \frac{ie^2 N \omega_0 c^2 \eta Z_{\parallel}}{2\omega_s E_0 C^2} . \quad (14.54)$$

If the impedance is a narrow resonance of centered at  $\omega_r$  near  $q\omega$ , only two terms contributes to  $\Re Z_{\parallel}$ :

$$\Re Z_{\parallel} \approx \frac{\omega_r}{\omega_0} [\Re Z_0^{\parallel}(\Omega + p\omega_0) - \Re Z_0^{\parallel}(p\omega_0 - \Omega)] , \quad (14.55)$$

where the coherent frequency  $\Omega$  is close to the synchrotron frequency  $\omega_s$ . Above transition ( $\eta > 0$ ), this leads to stability/instability if the resonance peak leans towards the lower/upper synchrotron sideband, in agreement with Robinson stability criterion. So far no Landau damping has been included.

Suppose that the particles in the bunch has a distribution  $\rho(\omega_s)$  in synchrotron frequency, centering at  $\bar{\omega}_s$  with spread  $\Delta\omega_s$ . We solve for  $\tau(s)$  in Eq. (14.52). Then integrate with the distribution to get

$$\bar{\tau}(s) = -\frac{ie^2 N \eta B \omega_0 c^2 Z_{\parallel}}{2\bar{\omega}_s E_0 C^2} e^{-i\Omega s/v} \int d\omega_s \frac{\rho(\omega_s)}{\omega_s - \Omega - i\epsilon} . \quad (14.56)$$

Substituting the ansatz of Eq. (14.51), self-consistency leads to the relation

$$-\frac{ie^2 N \omega_0 v^2 \eta Z_{\parallel}}{2\bar{\omega}_s \beta^2 E_0 C^2 \Delta\omega_s} = \frac{1}{R(u)} , \quad (14.57)$$

with  $u = (\bar{\omega}_s - \Omega)/\Delta\omega_s$ . Thus, from Eq. (14.54), we can again write

$$-\frac{(\Delta\omega_s)_{\text{coh}}}{\Delta\omega_s} = \frac{1}{R(u)} . \quad (14.58)$$

Therefore, we can define

$$U + iV = -i \frac{(\Delta\omega_s)_{\text{coh}}}{\Delta\omega_{s\text{HWHM}}} = \frac{i}{\hat{R}(x)} = \frac{\hat{g}(u) + i\hat{f}(x)}{\hat{f}^2(x) + \hat{g}^2(x)} \quad \text{with} \quad u = x \frac{\Delta\omega_{s\text{HWHM}}}{\Delta\omega_s} . \quad (14.59)$$

The stability threshold curve in the  $U$ - $V$  plane is exactly the same as in the transverse bunch instability analyzed in the previous section. The Keil-Schnell like stability circle is

$$|(\Delta\omega_s)_{\text{coh}}| \lesssim \frac{1}{\sqrt{3}} (\Delta\omega_s)_{\text{HWHM}} F , \quad (14.60)$$

where  $(\Delta\omega_s)_{\text{HWHM}}$  is the half-width-at-half-maximum of the synchrotron frequency spread, and the form factors  $F$  for various distribution are exactly the same as given in Table 14.2.

The above example is a demonstration of Landau damping in the presence of Robinson stability or instability. Therefore, even if the rf resonant peak is shifted in the wrong way so that the beam is Robinson unstable, there is still Landau damping from the spread in synchrotron frequency that may be able to stabilize the beam. However, this will not help much because the synchrotron frequency spread is usually not large enough unless there is a higher-harmonic rf system.

## 14.6 Transverse Unbunched Beam Instabilities

Consider an unbunched beam containing  $N$  particles oscillating in the transverse plane. The beam has a transverse dipole  $D(s, t)$  density (per unit longitudinal length) which depends on the location  $s$  along the ring and also time  $t$ . This is in fact the perturbed part of the beam: i.e., with the stationary distribution subtracted. Assume the ansatz

$$D(s, t) = \frac{eN}{C} \langle y(s, t) \rangle = \frac{eN\Delta}{C} \exp \left( i \frac{n}{R} s - i\Omega t \right) . \quad (14.61)$$

where  $\Delta$  is the maximum transverse deviation,  $n$  is a revolution harmonic,  $R = C/(2\pi)$  is the ring mean radius, and  $\Omega$  is the coherent frequency to be determined. This is a

snapshot view of the deviation of the perturbed beam and therefore must be a periodic function of the ring circumference. The ansatz in Eq. (14.61) assumes that the revolution harmonics are not related and each one can be studied independently.

A test particle at a fixed location  $s$  along the ring experiences a transverse force left by the dipole wave. At time  $t$ , this force is

$$\langle F_{\perp}(s, t) \rangle = -\frac{e}{C} \int_t^{\infty} v dt' W_1(vt' - vt) D(s, t') = \frac{iev\beta D(s, t) Z_1^{\perp}(\Omega)}{C}, \quad (14.62)$$

where  $v = \beta c$  is the velocity of the beam particles. Since the impedance is at a fixed location, observing the dipole density of Eq. (14.61), the impedance at  $s$  will see the time variation only and sample only the frequency  $\Omega$  of the dipole wave. The impedance will have no knowledge about the harmonic variation of the wave around the ring. However, as will be shown below, the solution of  $\Omega$  does depend on the revolution harmonic.

For a particle inside the beam, the situation is different because it moves with the beam at velocity  $v$ . Consider the specific particle which passes the location  $S$  at time  $t = 0$ . Its location at a later time changes according to  $s = S + vt$ . Its transverse displacement  $y(s, t)$  is governed by the equation of motion,

$$\frac{d^2y}{dt^2} + \omega_{\beta}^2 y = \frac{\langle F(S + vt, t) \rangle}{\gamma m} = \frac{ie^2 N c Z_1^{\perp}(\Omega) \Delta}{E_0 T_0^2} e^{inS/R - i(\Omega - n\omega_0)t}, \quad (14.63)$$

where  $E_0 = \gamma mc^2$  is the energy of the beam particle,  $m$  is its mass and  $T_0$  is revolution period. Although the impedance is still sampling the frequency  $\Omega$ , the transverse motion of the particle is driven by a force at the frequency  $\Omega - n\omega_0$ , with  $\omega_0 = v/R$  denoting the revolution angular frequency of the particle around the ring. It is important to point out that the time derivative in this equation is the *total* time derivative, because we are studying the particle displacement while traveling with the particle longitudinally. That explains why we have substituted  $s = S + vt$  in the exponent on the right hand side. In order to have a clearer picture, let us travel with the particle longitudinally and at the same time count the number of transverse oscillations the particle makes in a revolution turn. The result is the incoherent tune of the particle  $\nu_{\beta}$ , which equals  $(\Omega - n\omega_0)/\omega_0$ . On the other hand, from a beam-position monitor (BPM) at a fixed location monitoring the transverse motion of the particle, what it measures is the frequency  $\Omega$  or the residual betatron tune (the fractional part of the betatron tune) of the particle.

This force-driven differential equation (14.63) can be solved easily, giving the solu-

tion

$$[\omega_\beta^2 - (\Omega - n\omega_0)^2] y(s, t) = \frac{ie^2 N c Z_1^\perp(\Omega) \Delta}{E_0 T_0^2} e^{inS/R - i(\Omega - n\omega_0)t}. \quad (14.64)$$

Self-consistency requires  $y(s, t) = \Delta e^{i(ns/R - \Omega t)}$ , which cancels the exponential on both sides. For small perturbation, there are two solutions for the coherent frequency,  $\Omega \approx n\omega_0 \pm \omega_\beta$ . For a coasting beam, when we are talking about positive and negative revolution harmonics, we will arrive at the same physical conclusion when we choose either  $n\omega_0 + \omega_\beta$  or  $n\omega_0 - \omega_\beta$ . This is because (1) the beam spectra of the two choices are related by symmetry and (2)  $Z_1^\perp(\omega)$  has definite symmetry about  $\omega = 0$ . This reminds us of the similar situation when we studied synchrotron sidebands in Chapter 7. However, one must be aware that for a bunch beam, there will be synchrotron sidebands around the betatron line and the beam spectrum will no longer possess this property. With the convention in Fig. 10.1 or Eq. (10.17), we need to choose the positive sign, or there is only upper betatron sidebands. This leads us to the coherence betatron tune shift of the beam

$$(\Delta\omega_\beta)_{coh} = \Omega - (n\omega_0 + \omega_\beta) \approx -\frac{ie^2 N c}{2\omega_\beta E_0 T_0^2} Z_1^\perp(n\omega_0 + \omega_\beta). \quad (14.65)$$

The imaginary part of the transverse impedance provides a true betatron tune shift. The real part,  $\Re Z_1^\perp$ , however, will lead to damping/instability if the frequency sampled by the impedance is positive/negative. Actually when  $n\omega_0 + \omega_\beta = (n + \nu_\beta)\omega_0 < 0$ , we write  $n + \nu_\beta = -(|n| - \nu_\beta)$  so that the betatron line appears to be the lower sideband of the positive harmonic  $|n|$ . Thus, we have the conclusion that the beam is stable when a sharp resonance is driving at the upper sideband and unstable when it is driving at the lower sideband. Here, one must be careful that not all *upper* sidebands of a negative revolution harmonics will become *lower* sidebands in the language of positive frequency and hence can be unstable. This is because the betatron tune  $\nu_\beta = \nu_\beta^I + [\nu_\beta]$  has an integer part  $\nu_\beta^I$  and a residual (or decimal) part  $[\nu_\beta]$ . The *upper* sideband of the harmonic  $n$  can be unstable<sup>†</sup> only if  $(n + \nu_\beta^I) < 0$ .

To introduce Landau damping, let us allow a distribution  $\rho(\omega_\beta)$  in betatron frequency among the beam particles. The distribution is centered at  $\bar{\omega}_\beta$  with a narrow spread  $\delta\omega_\beta$ . From Eq. (14.65) we obtain the dispersion relation

$$1 = \frac{ie^2 N c Z_1^\perp(\Omega)}{2\bar{\omega}_\beta E_0 T_0^2} \int d\omega_\beta \frac{\rho(\omega_\beta)}{\omega_\beta - (\Omega - n\omega_0)}. \quad (14.66)$$

---

<sup>†</sup>There is no such complexity with the synchrotron sidebands, because the synchrotron tune does not have an integer part.

This is a dispersion relation because it gives the relation between the wave number  $n/R$  and frequency  $\Omega$ . Or

$$-\frac{(\Delta\omega_\beta)_{\text{coh}}}{\Delta\omega_\beta} = \frac{1}{R(u)} , \quad (14.67)$$

where  $u = (\bar{\omega}_\beta - \Omega - n\omega_0)/\Delta\omega_\beta$ . This relation is exactly the same as Eq. (14.42). The only difference is the dependence of the coherent betatron tune shift on impedance is different. Thus, we have also the Keil-Schnell like stability threshold

$$(\Delta\omega_\beta)_{\text{coh}} \lesssim \frac{1}{\sqrt{3}} (\Delta\omega_\beta)_{\text{HWHM}} F . \quad (14.68)$$

Some comments are in order.

1. In the dispersion relation of Eq. (14.66), the solution gives, for small driving impedance,  $\Omega \approx (n + \nu_\beta)\omega_0$ . Depending on whether  $n + \nu_\beta^I$  is positive or negative, this corresponds to two different dipole waves, one with a higher velocity is called the *fast wave*, while the one with a lower velocity is called the *slow wave*. As per discussion above, only the slow wave will lead to beam instability.
2. We have introduced a spread of the betatron frequency in order to arrive at Landau damping. In fact, the revolution frequency  $\omega_0$  in the denominator of the integrand of Eq. (14.66) also has a spread and can therefore contribute to Landau damping. Instead of the betatron frequency distribution  $\rho(\omega_\beta)$ , it will be more general to introduce the particle momentum distribution  $\rho(\delta)$ . We can develop the local betatron frequency up to the terms linear in the fractional momentum spread  $\delta$ :

$$(n + \nu_\beta)\omega_0 = (n + \bar{\nu}_\beta)\bar{\omega}_0 + [\xi - (n + \bar{\nu}_\beta)\eta]\bar{\omega}_0\delta , \quad (14.69)$$

where  $\xi$  is the chromaticity and  $\eta$  the slip factor in the longitudinal phase space, while  $\bar{\nu}_\beta$  and  $\bar{\omega}_0$  represent the nominal betatron tune and revolution frequency. For the dangerous slow wave, let us denote  $\hat{n} = -(n + \nu_\beta^I)$  where  $\hat{n} > 0$ . The above leads to

$$\Delta(n + \nu_\beta)\omega_0 = [\xi + (\hat{n} - [\bar{\nu}_\beta])\eta]\bar{\omega}_0\delta . \quad (14.70)$$

The integral in the dispersion relation becomes

$$\int d\omega_\beta \frac{\rho(\omega_\beta)}{\omega_\beta - (\Omega - n\omega_0)} \rightarrow \int d\delta \frac{\rho(\delta)}{[\xi + (\hat{n} - [\bar{\nu}_\beta])\eta]\bar{\omega}_0\delta - \hat{\Omega}} , \quad (14.71)$$

with  $\hat{\Omega} = \Omega - (n + \bar{\nu}_\beta)\bar{\omega}_0$ . One immediate conclusion is that when the chromaticity is negative and the ring is operating above transition ( $\eta > 0$ ), it may happen for some  $\hat{n}$  that  $\xi + (\hat{n} - [\bar{\nu}_\beta])\eta \approx 0$ . When this happens there will not be any Landau damping at all. The same is true for a positive chromaticity below transition. The dispersion relation can be rewritten as

$$-\frac{(\Delta\omega_\beta)_{\text{coh}}}{[\xi + (\hat{n} - [\bar{\nu}_\beta])\eta]\bar{\omega}_0\Delta\delta} = \frac{1}{R(u)} , \quad (14.72)$$

where

$$u = \frac{1}{\Delta\delta} \left[ \bar{\delta} - \frac{\hat{\Omega}}{[\xi + (\hat{n} - [\bar{\nu}_\beta])\eta]\bar{\omega}_0} \right] , \quad (14.73)$$

$\Delta\delta$  is the spread in momentum spread, and  $\bar{\delta}$  (usually zero) is the momentum spread where the distribution  $\rho(\delta)$  peaks at. The Keil-Schnell like stability threshold becomes

$$(\Delta\omega_\beta)_{\text{coh}} \lesssim \frac{1}{\sqrt{3}} |\xi + (\hat{n} - [\bar{\nu}_\beta])\eta| \bar{\omega}_0 (\Delta\delta)_{\text{HWHM}} F , \quad (14.74)$$

which, with the help of the coherent betatron tune shift in Eq. (14.65), can be rewritten as

$$|Z_1^\perp| \lesssim \frac{4\pi\omega_\beta E_0}{\sqrt{3}eI_0c} |\xi + (\hat{n} - [\bar{\nu}_\beta])\eta| (\Delta\delta)_{\text{HWHM}} F . \quad (14.75)$$

Zotter [8] was the first to derive this Keil-Schnell like transverse stability criterion for a coasting beam. His numerical coefficient on the right side is 8 which is very close to our value of  $4\pi/\sqrt{3}$ . Of course, the spread in betatron tune can also come from the betatron oscillation amplitude, and this spread should also be included in Eq. (14.69) for a more complete description.

## 14.7 Longitudinal Unbunched Beam Instabilities

For the last three categories, the transverse bunched beam instabilities, the transverse unbunched beam instabilities, and the longitudinal bunched beam instabilities, the treatment had been very similar. In each case, we first derived the tune shifts. Landau damping was next introduced by including the distribution of the tune. The dispersion relation derived was related to the BTF  $R(u)$ , from which the stable and unstable regions in the impedance phase space could be identified. The longitudinal instabilities of an unbunched beam is very much different, because there is no stabilizing oscillation

like the betatron motion or synchrotron motion. Thus, there is no betatron frequency or synchrotron frequency, from which a coherent frequency spread can be obtained to provide Landau damping. As a result, the derivation of the stability criterion will be very different from the last three categories. Here, the collective beam instability is the longitudinal microwave instability, and Landau damping is supplied by the spread in revolution frequency of the beam particles. The dispersion relation, Eq. (6.13), has been derived in Chapter 6 and the stability curves are shown in Fig. 6.4. Over there, the dispersion relation was derived employing the Vlasov equation which deals with the evolution of the particle distribution. We will show another derivation in this section making use of only the equations of motion without resorting to the Vlasov equation.

Let us start from the linear distribution  $\lambda(s, t)$  which has a stationary part  $\lambda_0$  and a perturbation  $\Delta\hat{\lambda}$ . The stationary part is just a uniform distribution

$$\lambda_0 = \frac{N}{C} , \quad (14.76)$$

where  $N$  is the total number of particles in the unbunched beam. For the perturbation, we postulate the ansatz

$$\Delta\lambda(s, t) = \Delta\hat{\lambda}e^{ins/R-i\Omega t} , \quad (14.77)$$

where  $\Delta\hat{\lambda}$  represents the maximum modulation of the longitudinal density and is assumed to be small, and the harmonic  $n = 0$  is excluded because of charge conservation. A snapshot view at a specific time will show the  $n$ -fold modulation of the linear density.

For a test particle at the fixed location  $s$ , the average longitudinal force experienced from the longitudinal wave is

$$\langle F(s, t) \rangle = -\frac{e^2}{C} \int v dt' W'_0(vt - vt') \Delta\lambda(s, t') = -\frac{e^2 v Z_0^{\parallel}(\Omega)}{C} \Delta\lambda(s, t) , \quad (14.78)$$

where the impedance only samples the collective frequency  $\Omega$ .

Next consider a particle moving with the beam. It passes the location  $S$  at time  $t = 0$  and is at location  $s = S + vt$  at later time  $t$ . The motion of a beam particle consists of its phase drift and energy drift in the longitudinal phase space. The particle's off-momentum spread  $\delta(s, t)$  increases per unit time as a result of the wake force and is governed by

$$\frac{d\delta(s, t)}{dt} = -\frac{e^2 c^2}{CE} Z_0^{\parallel}(\Omega) \Delta\hat{\lambda} e^{ins/R-i\Omega t} . \quad (14.79)$$

while the rate of the phase drift is governed by

$$\frac{dz(s, t)}{dt} = -\eta v \delta(s, t) , \quad (14.80)$$

where  $\eta$  is the slip parameter and we have actually employed a distance drift  $z(s, t)$  rather than a phase. Here,

$$\frac{d}{dt} = \frac{\partial}{\partial t} + \frac{ds}{dt} \frac{\partial}{\partial s} \quad (14.81)$$

is the *total* time derivative. Thus, in solving Eqs. (14.79) and (14.80), we must first make the substitution  $s = S + vt$ . The momentum-offset equation can be integrated readily to give

$$\delta(s, t) = \frac{e^2 c^2}{CE} Z_0^{\parallel}(\Omega) \Delta \hat{\lambda} \frac{e^{ins/R-i\Omega t}}{i(\Omega - n\omega_0)} . \quad (14.82)$$

Substituting the result into the phase-drift equation, we obtain by another integration

$$z(s, t) = -\frac{e^2 \eta c^2 v}{CE_0} Z_0^{\parallel}(\Omega) \Delta \hat{\lambda} \frac{e^{ins/R-i\Omega t}}{(\Omega - n\omega_0)^2} . \quad (14.83)$$

Notice that in the above solution we have kept only the contribution due to the wake field.

If we can relate the particle longitudinal displacement  $z(s, t)$  to the longitudinal density perturbation  $\Delta\lambda$ , the loop will be closed in Eq. (14.83) and a dispersion relation will result. There is in fact such a relation from the equation of continuity. The particles in the original unperturbed volume from  $s$  to  $s + \Delta s$  at time  $t$  are displaced into the new perturbed volume between  $s + z(s, t)$  and  $s + \Delta s + z(s + \Delta s, t)$  at time  $t$  in the presence of the wake force. The number of particles in each of the volumes is

$$\lambda_0 ds = [\lambda_0 + \Delta\lambda(s, t)] \left\{ [s + \Delta s + z(s + \Delta s, t)] - [s + z(s, t)] \right\} , \quad (14.84)$$

from which we obtain, for small  $\Delta s$ ,

$$\Delta\lambda(s, t) = -\lambda_0 \frac{\partial z}{\partial s} = \frac{ineI_0 \eta \omega_0^2 Z_0^{\parallel}(\Omega)}{2\pi\beta^2 E_0} \Delta \hat{\lambda} \frac{e^{ins/R-\Omega t}}{(\Omega - n\omega_0)^2} , \quad (14.85)$$

where we have introduced the average beam current  $I_0 = eN\omega_0/(2\pi)$  with  $\omega_0 = v/R$  being the angular revolution frequency. Self-consistency allow us to cancel  $\Delta\lambda(s, t)$  on both sides. The growth rate of the longitudinal wave  $\omega_G$  is given by the imaginary part of  $\Omega$ , which can be readily obtained from Eq. (14.85),

$$\omega_G^2 = -\frac{ieI_0 Z_0^{\parallel}(\Omega) n \eta}{2\pi\beta^2 E_0} \omega_0^2 , \quad (14.86)$$

which is very similar to the definition of the synchrotron frequency, if we identify the rf voltage as  $I_0 Z_0^{\parallel}$  and the rf harmonic as  $n$ . For this reason, the growth rate can be visualized as the synchrotron angular frequency inside a bucket created by the voltage the beam experiences from the impedance. We can draw the immediate condition that the longitudinal wave perturbation is stable above/below transition ( $\lessgtr$ ) only if the impedance is purely inductive/capacitive.

Landau damping can now be introduced by allowing a spread in the revolution frequency inside the beam. Let  $\rho(\omega_0)$  be the distribution in revolution frequency centering at  $\bar{\omega}_0$  with a spread  $\Delta\omega_0$ . Multiplying both sides of Eq. (14.85) by  $\rho(\omega_0)$  and integrating over  $d\omega_0$ , we obtain the dispersion relation

$$1 = \frac{ieI_0 Z_0^{\parallel}(\Omega)n\eta}{2\pi\beta^2 E_0} \int d\omega_0 \frac{\rho(\omega_0)}{(\Omega - n\omega_0 + i\epsilon)^2}. \quad (14.87)$$

The dispersion relation can be rewritten as

$$1 = \left[ \frac{\omega_g^2}{n^2(\Delta\omega_0)^2} \right] \left[ n(\Delta\omega_0)^2 \int d\omega_0 \frac{\rho'(\omega_0)}{n\omega_0 - \Omega - i\epsilon} \right] = \left[ \frac{\omega_g^2}{n^2(\Delta\omega_0)^2} \right] R_{\parallel}(u), \quad (14.88)$$

where an integration by part has been performed. The function  $R_{\parallel}$  on the right is defined as

$$R_{\parallel}(u) = f_{\parallel}(u) + ig_{\parallel}(u) = (\Delta\omega_0)^2 \left[ \wp \int d\omega_0 \frac{\rho'(\omega_0)}{\omega_0 - \Omega/n} + i\pi\rho' \left( \frac{\Omega}{n} \right) \right], \quad (14.89)$$

and

$$u = \frac{\bar{\omega}_0 - \Omega/n}{\Delta\omega_0}. \quad (14.90)$$

Usually one writes

$$V - iU = \frac{\omega_g^2}{n^2(\Delta\omega_0)^2} = \frac{f_{\parallel}(u) - ig_{\parallel}(u)}{f_{\parallel}^2(u) + g_{\parallel}^2(u)}, \quad (14.91)$$

so that  $U \propto -\mathcal{Re} Z_0^{\parallel}$  and  $V \propto -\mathcal{Im} Z_0^{\parallel}$ . This will give the threshold and growth curves for longitudinal microwave instability in Chapter 6.

## 14.8 Beam Transfer Function and Impedance Measurements

Consider a coasting beam. In addition to the transverse wake, if we give an extra sinusoidal kick with harmonic  $n$  and frequency  $\Omega$ , the equation of motion is

$$\ddot{y} + \omega_\beta^2 y = -2(\Delta\omega_\beta)_{\text{coh}}\omega_\beta \langle y \rangle + A e^{ins/R-i\Omega t}, \quad (14.92)$$

where the coherent betatron tune shift  $(\Delta\omega_\beta)_{\text{coh}}$  is given by Eq. (14.37). For the particular solution, try the ansatz

$$\langle y(s, t) \rangle = B e^{ins/R-i\Omega t}. \quad (14.93)$$

As before,  $s = S + vt$ , and we obtain

$$y(s, t) = \frac{[-2(\Delta\omega_\beta)_{\text{coh}}\omega_\beta B + A] e^{ins/R-i\Omega t}}{\omega_\beta^2 - (n\omega_0 - \Omega)^2}. \quad (14.94)$$

Consistency requires

$$B \approx \frac{-2(\Delta\omega_\beta)_{\text{coh}}\omega_\beta B + A}{2\omega_\beta} \int d\omega \frac{\rho(\omega)}{\omega - (\Omega - n\omega_0)} = \frac{-2(\Delta\omega_\beta)_{\text{coh}}\omega_\beta B + A}{2\omega_\beta \Delta\omega} R(u), \quad (14.95)$$

and after rearranging,

$$\frac{A}{2\omega_\beta \Delta\omega B} = \frac{1}{R(u)} + \frac{(\Delta\omega_\beta)_{\text{coh}}}{\Delta\omega}. \quad (14.96)$$

In a measurement, the beam is kicked at a certain harmonic but with various frequencies  $\omega$  and the response is measured in its amplitude and phase. If the beam is of very weak intensity, the coherent tune shift term can be neglected and one can therefore obtain the BTF  $R(u)$ . Next, the beam intensity is increased to such a large value that the beam is still stable. The measurement of the beam response will give a stability curve shifted by  $(\Delta\omega_\beta)_{\text{coh}}/\Delta\omega$ . From the shift one can infer the impedance  $Z_1^\perp$  of the vacuum chamber as illustrated in the left plot of Fig. 14.6

For the longitudinal BTF, we add a longitudinal kicking voltage per unit length,  $A$  with revolution harmonic  $n$  and frequency  $\Omega$ . Then the longitudinal force seen by a particle changes from Eq. (14.78) to

$$\langle F(s, t) \rangle = -\frac{e^2}{C} \int v dt' W'_0(vt - vt') \Delta\lambda(s, t) \rho(\omega_0) + A e^{ins/R-i\Omega t}. \quad (14.97)$$

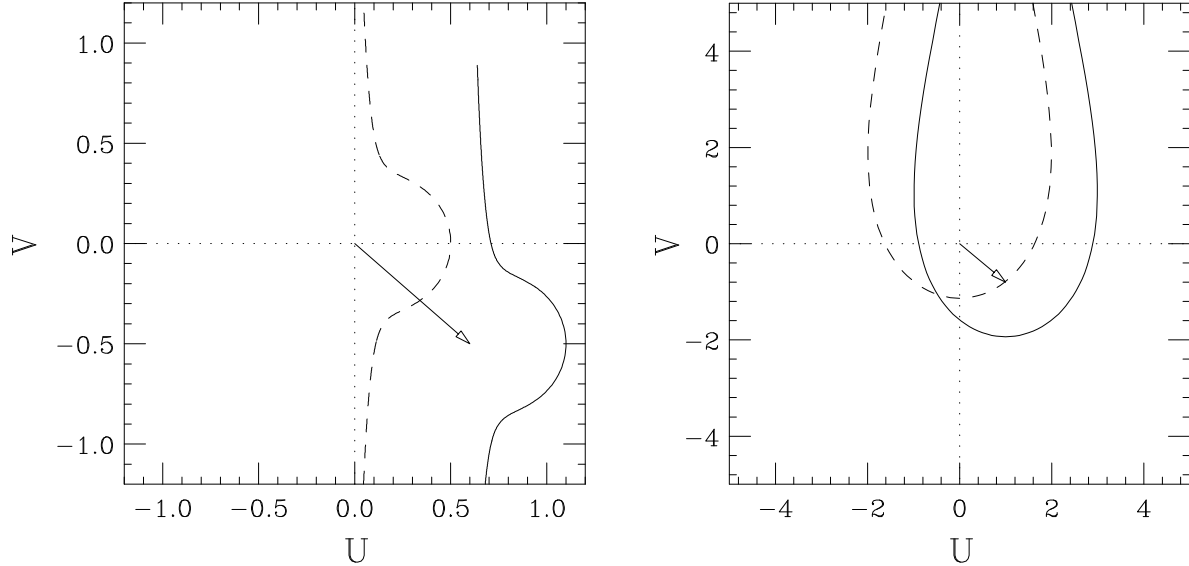


Figure 14.6: Left: Transverse beam response function of a coasting beam. Dash curve is for a very low-intensity beam, thus showing the threshold curve. But it is shifted to the solid curve at high intensity. The transverse impedance can be inferred from the shift indicated by the arrow. Right: Longitudinal beam response function of a coasting beam. The dashed curve is for low intensity and is shifted to the solid curve at high intensity. The arrow is proportional to the longitudinal impedance.

Assume the ansatz

$$\Delta\lambda(s, t) = Be^{ins/R - i\Omega t}. \quad (14.98)$$

Then the solution of the momentum spread and longitudinal drift become

$$\delta(s, t) = \frac{-e^2 c^2}{CE} Z_0^{\parallel}(\Omega) B + A \frac{e^{ins/R - i\Omega t}}{-i(\Omega - n\omega_0)}. \quad (14.99)$$

$$z(s, t) = \eta v \frac{-e^2 c^2}{CE} Z_0^{\parallel}(\Omega) B + A \frac{e^{ins/R - i\Omega t}}{(\Omega - n\omega_0)^2}. \quad (14.100)$$

Doing the same as Eqs. (14.85) and (14.87), we obtain

$$B = \left[ \frac{\omega_g^2}{n^2(\Delta\omega)^2} B + \frac{i2\pi\eta v N}{n^2(\Delta\omega)^2 C^2} A \right] R_{\parallel}(u). \quad (14.101)$$

Or,

$$\frac{i2\pi\eta v N}{n^2(\Delta\omega)^2 C^2} \frac{A}{B} = \frac{1}{R_{||}(u)} - \frac{\omega_g^2}{n^2(\Delta\omega)^2}. \quad (14.102)$$

Exactly in the same way as the transverse counterpart, for a very low-intensity beam, the response of the kick gives the threshold curve. For an intense beam, this threshold curve will be shifted. The amount and direction of shift will be proportional to the magnitude and phase of the longitudinal impedance. This is shown in the right plot of Fig. 14.6.

BTF and impedance measurements have been attempted by Spentzouris [9] at the Fermilab Accumulator Antiproton Storage Ring. The Accumulator stores antiprotons at  $E_0 = 8.696$  GeV with an rms spread of  $1-4 \times 10^{-4}$ . The ring has a revolution frequency  $f_0 = 628.955$  kHz and a slip parameter  $\eta = 0.023$ . There are 3 rf cavities in the ring, ARF2 and ARF3 are at rf harmonic  $h = 2$ . The third one ARF1 at rf harmonic 84 has been used as a kicker. The impedance of cavity ARF3 was the target for measurement. The hardware setup for the BTF measurement is shown in Fig. 14.7. The network

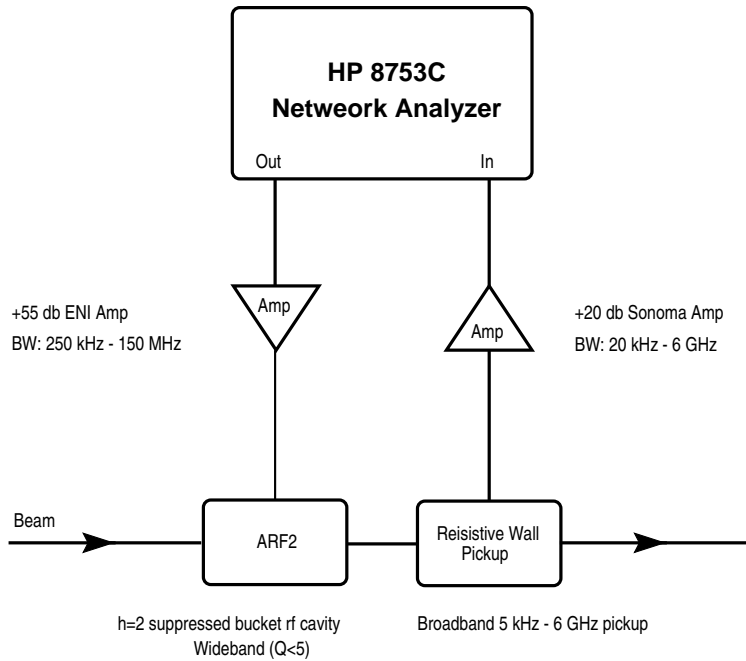


Figure 14.7: Block diagram of Accumulator transfer function measurement setup.

analyzer excited the beam longitudinally by applying a swept frequency of sinusoidal wave to the broadband cavity ARF2 (quality factor  $Q < 5$ ). The resulting frequency

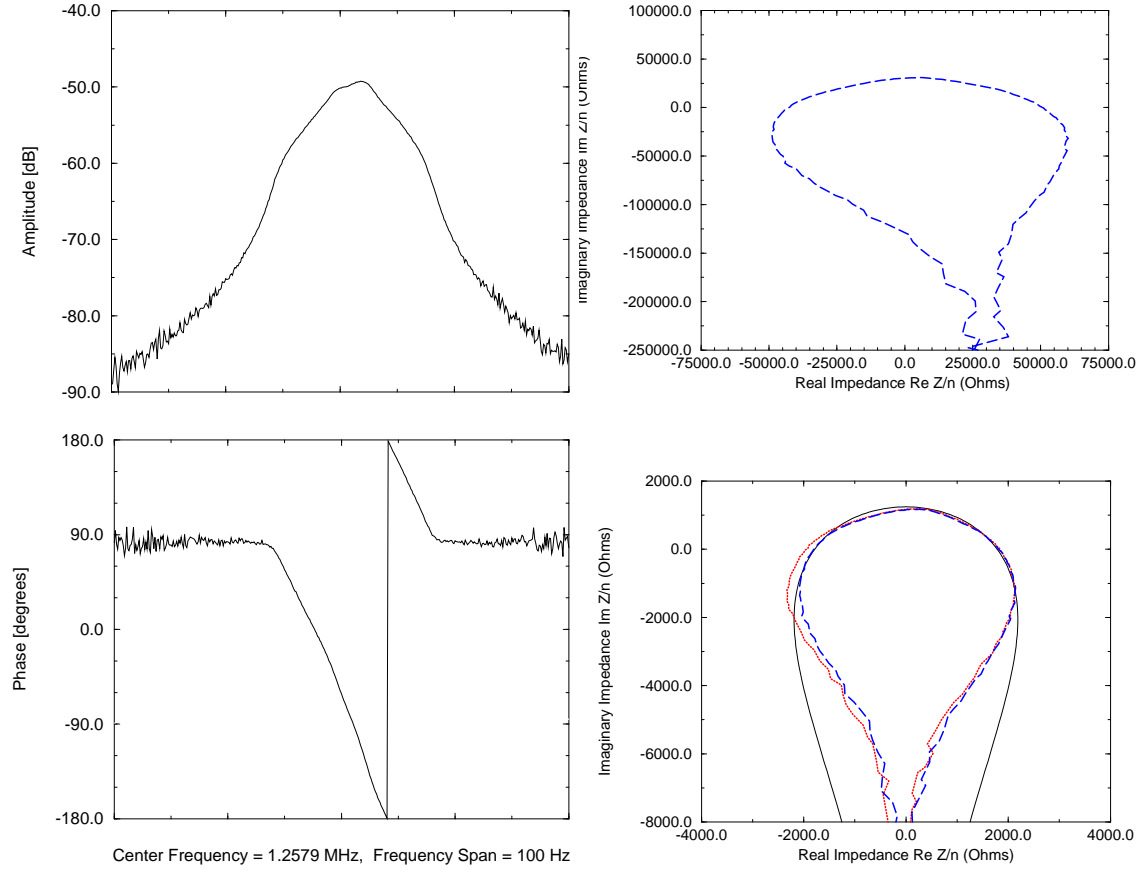


Figure 14.8: (color) Top left and bottom left: Amplitude and phase response of  $S_{21}$  measurement at  $h = 2$  in the Accumulator with cavity ARF3 shorted mechanically. Frequency sweeps were injected at cavity ARF2. Beam parameters: intensity 68 mA and energy 8.696 GeV with rms spread 2.6 MeV. Network analyzer setup: 401 data points, sweep time 41 s, and resolution bandwidth 10 Hz. Top right: Un-calibrated stability threshold curve from data displayed at the left. Bottom right: Same stability threshold curve (blue dashes) as in above, but fitted to the theoretical threshold curve (solid) after scaling and rotational corrections. Dotted red curve shows another set of measurement.

response of the beam picked up by a resistive wall monitor was directed to the return port of the analyzer.

Cavity ARF3 was first shorted mechanically and the signals of the beam response of the frequency sweep was monitored. A typical BTF measurement is shown in two left plots of Fig. 14.8, where the sweep was centered at  $2f_0 = 1.25791$  MHz with a span of 100 Hz which was wide enough to encompass the frequency content of the beam.

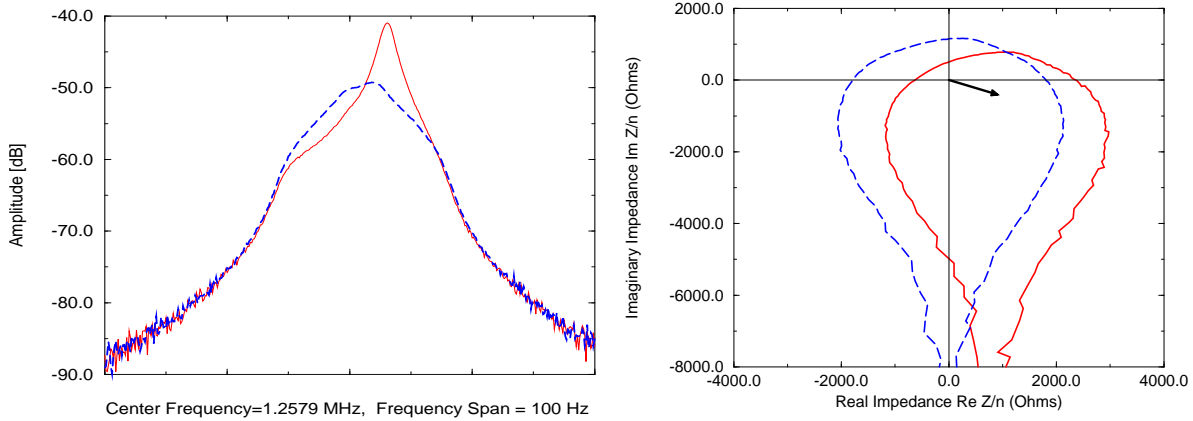


Figure 14.9: (color) Left: BTF measurements of the Accumulator with the ARF3 cavity shorted mechanically (blue-dashes) and with the mechanical short removed (solid red). Right: Stability threshold curves in the impedance complex plane with the ARF3 cavity shorted mechanically (blue-dashes) and with the mechanical shorts removed (solid red). The shift, indicated by the arrow, is the impedance per harmonic of the ARF3 cavity. The origin of the threshold curve with shorts out is shifted by approximately  $(x, y) = (900, -390)$   $\Omega$ , which gives an ARF3 cavity impedance of  $Z_0^{\parallel}/n = 490 \pm 110 \Omega$  with a phase angle of  $-23^\circ$ .

Notice that the response monitored shows more uncertainty at both ends of the sweep because of the decreasing particle population at those outlying frequencies. The setup of the network analyzer were 401 data points, sweep time 41 s, and resolution bandwidth 10 Hz. Inverting the BTF gives the stability threshold curve of the Accumulator as depicted in top right plot of Fig. 14.8. A series of corrections were made to convert this uncalibrated threshold curve to the one in blue dashes in the bottom right plot. This includes scaling, rotation, and fitting to the central part of the theoretical threshold curve which is shown as solid in the same plot. The red dotted curve is the result of another set of sweep measurement.

The mechanical shorts in cavity ARF3 were removed and the BTF measurement repeated. The frequency response or the BTF is shown in solid red in the left plot of Fig 14.9. The original BTF with the ARF3 shorted (top left plot of Fig 14.8) is also shown in blue dashes for comparison. The BTF's are inverted and are displaced in the impedance complex plane in the right plot of Fig 14.9. The calibrated threshold curve is shifted from the one with the mechanical shorts (blue dashes) to the one without the mechanical shorts (red solid). The shift represented by the arrow is the impedance per unit harmonic of the ARF3 cavity:  $Z_0^{\parallel}/n = 490 \pm 110 \Omega$  with a phase angle of  $-23^\circ$ .

## 14.9 Exercises

- 14.1. A shock excitation is given to a bunch with a Lorentz frequency distribution  $\rho(\omega)$  so that at  $t = 0$  each particle has  $\dot{x}(t) = \dot{x}_0$ . Compute the response of the displacement of the center of the bunch  $\langle x(t) \rangle$  and show that it does not decay to zero. Show that this is because  $\rho(0) \neq 0$ .
- 14.2. Derive the shock response function  $G(t)$  and beam transfer function  $R(u)$  for the various frequency distributions as listed in Table 14.1. Fill in those items that have been left blank.
- 14.3. Derive the  $U$ -intercept and the form factor  $F$  defined in Eq. (14.49) for various distributions as listed in Table 14.2.



# Bibliography

- [1] L.D. Landau, J. Phys. USSR **10**, 25 (1946).
- [2] J.D. Jackson, Nuclear Energy Part C: Plasma physics **1**, 171 (1960).
- [3] V.K. Neil and A.M. Sessler, Rev. Sci. Instr. **6**, 429 (1965).
- [4] L.J.Laslett, V.K. Neil, and A.M. Sessler, Rev. Sci. Instr. **6**, 46 (1965).
- [5] H.G. Hereward, CERN Report 65-20 (1965).
- [6] A. Hofmann, *Frontiers of Part. Beams: Intensity Limitations*, Hilton Head Island, Lecture in Phys. **400**, Springer-Verlag, 1990, p.110.
- [7] A.W. Chao, *Physics of Collective Beam Instabilities in High Energy Accelerators*, Wiley Interscience, 1993, Chapter 5.
- [8] B. Zotter and F. Sacherer, *Transverse instabilities of Relativistic Particle Beams in Accelerator and Storage Rings*, Proceedings of the First Course of the International School of Particle Accelerators of the ‘Ettore Majorana’ Centre for Scientific Culture, Erice, 10-22 November 1976, p.176.
- [9] L.K. Spentzouris, *Coherent Nonlinear Longitudinal Phenomena in Unbunched Synchrotron Beams*, Phd Thesis, Northwestern University, 1996.

